

Evidential Uncertainty Sets in Deep Classifiers Using Conformal Prediction

Hamed Karimi

HAMED.KARIMI@TORONTOMU.CA

Department of Electrical, Computer, and Biomedical Engineering, Toronto Metropolitan University, Toronto, ON, Canada

Reza Samavi

SAMAVI@TORONTOMU.CA

Department of Electrical, Computer, and Biomedical Engineering, Toronto Metropolitan University, Toronto, ON, Canada

Vector Institute, Toronto, ON, Canada

Abstract

In this paper, we propose *Evidential Conformal Prediction (ECP)* method for deep classifiers to generate the conformal prediction sets. Our method is designed based on a non-conformity score function that has its roots in Evidential Deep Learning (EDL) as a method of quantifying model (epistemic) uncertainty in DNN classifiers. We use evidence that are derived from the logit values of target labels to compute the components of our non-conformity score function: the heuristic notion of uncertainty in CP, uncertainty surprisal, and expected utility. Our extensive experimental evaluation demonstrates that ECP outperforms three state-of-the-art methods for generating CP sets, in terms of their set sizes and adaptivity while maintaining the coverage of true labels.

Keywords: Conformal Prediction; Uncertainty Quantification; Evidential Deep Learning; Model Confidence; Deep Neural Networks;

1. Introduction

Uncertainty Quantification (UQ) in Deep Neural Networks (DNNs) plays a crucial role in safety-critical applications, such as medical diagnosis (Vazquez and Facelli, 2022) and robotics (Tonkens et al., 2023). Conformal Prediction (CP) or Conformal Inference (Vovk et al., 2005; Papadopoulos et al., 2002) is a distribution-free, post-processing framework for UQ in image classification with promising properties such as no assumption on input data distribution, types of the pretrained model architecture, and domain of application. Rather than providing a single point prediction, CP constructs a finite *prediction set* or *uncertainty set* that encompasses a plausible subset of class labels for a given unseen input data point. In CP, three criteria are important to ensure the quality of the produced prediction sets: (1) the inclusion of the true labels, with a high probability, in the prediction set known as *coverage*, (2) the size of the set known as *efficiency* so that larger the set size, higher the model uncertainty, and (3) *adaptivity* in both former properties: adaptivity in set size, i.e. producing relatively larger sets for difficult examples compared to easy examples (e.g., a well-projected image of a bird is considered easier to classify than a cropped one), and coverage, i.e. having higher probability for inclusion of true label in the prediction set. A major challenge in CP research, is to construct high quality prediction sets where all these three properties are well maintained.

To address this challenge, a *non-conformity score* function is considered in CP to find an optimal probability threshold for inclusion of a label in the prediction sets. The score represents a measure of discrepancy between model predictive outcomes and true labels. The score is used to compare an unseen data point in a validation dataset with those in a relatively smaller calibration set (e.g., 500 examples) called the holdout dataset. The selection of this score function is arbitrary as long as it meets coverage property, yet the function plays a crucial role in meeting the other two properties when generating a prediction set: efficiency and adaptivity. For image classification tasks, two state-of-the-art (SoTA) CP methods are proposed with different non-conformity score functions, each addressing one or more CP properties. The *Adaptive Prediction Set (APS)* approach (Romano et al., 2020) prioritizes adaptivity over efficiency by producing larger prediction sets (inefficient) using cumulative summation of sorted softmax probabilities in its non-conformity function. To further improve efficiency, *Regularized Adaptive Prediction Sets (RAPs)* approach (Angelopoulos et al., 2020) regularizes APS’s non-conformity scores to reduce the set size by penalizing the softmax probabilities for unlikely labels with two constant hyperparameters.

In this paper, we propose *Evidential Conformal Prediction (ECP)* as a CP method for image classifiers, with a non-conformity score function that better maintains CP properties compared to SoTA methods. Our approach has its roots in Evidential Deep Learning (EDL) (Sensoy et al., 2018) as a method of quantifying model (epistemic) uncertainty in DNN classifiers. We use this uncertainty as our heuristic notion of uncertainty and produce rigorous uncertainty using our proposed CP method. In our non-conformity function, the scores are computed based on the evidence derived from logit values of target labels. We map the evidence to belief masses, which are the probabilities indicating the amount of confidence on each label being the true label. The belief masses are used to compute our heuristic uncertainty. We also use evidence to compute parameters of a Dirichlet distribution that produce the predictive probabilities associated with the target labels. These predictive probabilities along with our heuristic uncertainty are used to compute two evidential properties: *uncertainty surprisal* as the amount of information we still require to confidently predict the model outcomes, and *expected utility* as a distribution over target labels expressing the performance or effectiveness of a learning model. Then, we define and compute our non-conformity score function using these evidential properties. Our non-conformity scores are measurable without additional overhead. The coverage is theoretically guaranteed (Theorem 4), and as per our extensive experimental evaluations, the average empirical coverage is stochastically the same as the user-specified coverage level while producing adaptive and smaller (more efficient) prediction sets compared to SoTA methods.

We are making three contributions: (1) we introduce ECP with a novel non-conformity score function leading to efficient prediction sets while maintaining their coverage and adaptivity, (2) we propose a reliability metric to measure the confidence and uncertainty associated with the expected coverage, i.e. marginal coverage over unseen input data, and (3) we propose a quality metric for the prediction set based on violation from guaranteed coverage (as defined in (Angelopoulos et al., 2020)) and the average set size.

2. Related Work

In CP, there are SoTA methods to quantify model uncertainty either by generating a scaled value from the produced prediction sets to facilitate performing comparative evaluations with non-CP methods (Karimi and Samavi, 2023) or by improving the efficiency and adaptivity of prediction sets. A classical approach to generate prediction sets for unseen data is to include labels from the most likely to the least likely softmax probabilities until their cumulative summation exceeds the threshold $1 - \delta$. In this approach, the true label coverage cannot be guaranteed since the output probabilities are overconfident and uncalibrated (Nixon et al., 2019). Furthermore, the lower probabilities in image classifiers are significantly miscalibrated which gives rise to larger prediction sets that may misrepresent the model uncertainty. There are also a few methods to generate prediction sets, but not based on conformal prediction (Pearce et al., 2018; Zhang et al., 2018). However, these methods do not have finite marginal coverage guarantees as described in Theorem 4.

The coverage guarantee can be achieved using a new threshold and holdout data. In this regard, Romano et al. (Romano et al., 2020) proposed a method to make CP more stable in the presence of noisy small probability estimates in image classification. The authors developed a conformal method called APS to provide marginal coverage of true label in the prediction set which is also fully adaptive to complex data distributions using a novel conformity score, particularly for classification tasks. For example, with $\delta = 0.1$, if selecting prediction sets that contain 0.85 estimated probability can achieve 90% coverage on the holdout data, APS will utilize the threshold 0.85 to include labels in the prediction sets. However, APS still produces large prediction sets which cannot precisely represent the model uncertainty. To mitigate the large set size, the authors in (Angelopoulos et al., 2020) introduced a regularization technique called RAPS to relax the impact of the noisy probability estimates which yield to significantly smaller and more stable prediction sets. RAPS modifies APS algorithm by penalizing the small softmax scores associated with the unlikely labels after temperature scaling (Platt et al., 1999) using two hyperparameters k_{reg} and λ . RAPS regularizes the APS method, therefore, RAPS acts exactly as same as APS when setting the regularization parameter λ to 0. Both APS and RAPS methods are always certified to satisfy the marginal coverage in Equation (4) regardless of model, architecture, and dataset. Thus, RAPS could outperform APS by significantly smaller prediction sets. Thus, RAPS can produce adaptive but more efficient (smaller) prediction sets as an estimation of the model uncertainty given unseen image data samples. Both methods also require negligible computational complexity in both finding the proper threshold using the holdout data. However, both methods requires an optimization process to find optimal temperature and generate softmax scores as predictive probabilities. Moreover, RAPS requires another optimization process to find the optimal λ that generates the most adaptive sets while sacrificing the set size. These further optimization process may give rise to higher computational burden in RAPS. Another method to produce small sets is called Least Ambiguous Set-valued (LAS) introduced in (Sadinle et al., 2019). LAS produces small average set size in the case where the input probabilities are correct. However, compared to SoTA methods, LAS has higher violations from the desired exact coverage probability $1 - \delta$ conditional on ranges of set sizes.

There are also other methods to quantify model (epistemic) uncertainty in DNNs such as Bayesian (Gal and Ghahramani, 2016; Lakshminarayanan et al., 2016) and evidential (Sensoy et al., 2018; Amini et al., 2020) methods. (Sensoy et al., 2018) proposed the notion of Evidential Deep Learning (EDL) to quantify uncertainty in classification tasks and showed that their approach is robust for out-of-distribution testing data. EDL uses Dempster-Shafer Theory (DST) to produce evidence for target labels based on the logit values and maps the evidence to Dirichlet distribution parameters. EDL could effectively capture the epistemic uncertainty associated with classification tasks using Subjective Logic (SL) (Jøsang, 2016) as a framework that formalizes DST. In this paper, we exploit EDL originated in SL to devise our non-conformity score function in CP setting as described in the following sections.

3. Evidential Conformal Prediction

In the following sections, we formally describe Evidential Deep Learning in Section 3.1, the procedure of computing evidential properties in Section 3.2 as components of our proposed non-conformity score function leading to constructing efficient and adaptive prediction sets described in Sections 3.3 and 3.4 which is introduced as *Evidential Conformal Prediction (ECP)*. Finally, in Section 3.5, we discuss the confidence and uncertainty associated with the true label coverage after producing prediction sets.

3.1. Evidential Deep Learning

Dempster–Shafer Theory of Evidence (DST) generalizes Bayesian theory by individually assigning a probability called belief mass to each of the possible states of the model (e.g. model outcomes), thus, allowing DST to explicitly represent incomplete and partially reliable knowledge about the states. Belief masses are probabilities that are assigned to subsets of a frame of discernment (including the entire frame itself) that denotes a set of exclusive possible states (Dempster, 1968; Shafer, 1976). Belief masses represent the amount of confidence that the truth can be any of the possible states. For example, in a DNN classifier, any combination of assigned target labels are possible states of the model outcomes as each class label can be assigned by a probability as a *belief* mass to indicate the confidence on which class label is the true label. By assigning all belief masses to the entire possible model outcomes, the notion of “I do not know” can be expressed as the uncertainty that indicates lack of confidence over model outcomes (Jøsang, 2016). The Dempster-Shafer theory is restricted by ignoring the base rates or prior probabilities associated with the possible outcomes, the theory of subjective logic formalizes and extends the DST’s notion of belief assignments to each of the model outcomes by the inclusion of the base rates associated with target labels and mapping the evidence obtained from input data to belief masses using a Dirichlet distribution. Therefore, in subjective logic, belief masses are function of evidence. For example, in a DNN classifier, evidence can be computed based on the logit values to form belief masses. Note that the notion of evidence we are using in this proposal, is different from what considered as marginal likelihood in Bayesian models.

Evidential Deep Learning built on Dempster-Shafer theory and subjective logic, obtains the evidence from the logit values in a DNN, and maps the produced evidence to Dirichlet parameters in order to form a predictive Dirichlet distribution. Informally, *evidence* in

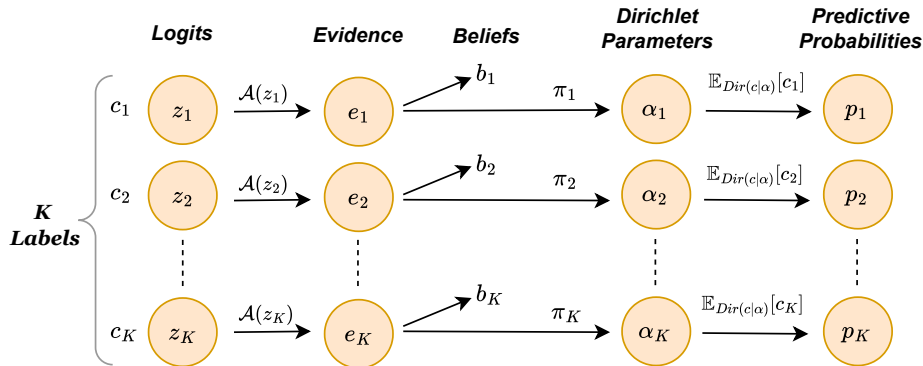


Figure 1: An overview of Evidential Deep Learning (EDL): For each data point, the evidence values are calculated based on logits to produce belief masses and Dirichlet parameters, and finally, achieving predictive probabilities.

evidential deep learning is the amount of support collected from input data in favor of classifying a data point into a specific label (Sensoy et al., 2018).

Definition 1 (Evidence in DNN) *In a classifier with K target labels, suppose z_k is the logit value associated with the label $k \in \{1, 2, \dots, K\}$ and $\mathcal{A} : \mathbb{R} \rightarrow \mathbb{R}^+$ is a non-linear non-negative activation function. Then, the non-negative real evidence e_k associated with the label k is defined as $e_k = \mathcal{A}(z_k)$.*

Definition 2 (Base Rate (Prior Probability) in DNN) *In a classifier with K target labels, the prior probability π_k associated with the label $k \in \{1, 2, \dots, K\}$ is called base rate and defined as the probability of each label being the true label in classifying a data point prior to any observation or training process.*

We illustrate the process of generating evidence, belief masses, and Dirichlet parameters from logit values in Figure 1. Formally, we replace the softmax layer with an activation layer (non-linear non-negative activation function \mathcal{A} , e.g. ReLU function), corresponding to a latent categorical distribution $\mathbf{c} = \{c_1, c_2, \dots, c_K\}$ denoting the probabilities associated with target labels $\mathcal{Y} = \{1, 2, \dots, K\}$. When classifying a data point, the activation function \mathcal{A} is applied to logit values z_k associated with target labels $k \in \mathcal{Y}$ to produce real non-negative evidence values denoted by $e_k \in \mathbf{E}$ for each label k . Note that $\mathbf{E} = \{e_k \mid k \in \mathcal{Y}\}$ denotes the set of evidence associated with target labels in \mathcal{Y} . Following Definition 1 (evidence) and Definition 2 (base rate), now we can form a Dirichlet distribution with the parameter set $\boldsymbol{\alpha} = \{\alpha_k \mid k \in \mathcal{Y}\}$ by computing its corresponding Dirichlet parameters $\alpha_k \in \boldsymbol{\alpha}$ based on the corresponding evidence e_k and the base rates π_k as,

$$\alpha_k = e_k + K \cdot \pi_k \implies \alpha_k = e_k + 1, \quad (1)$$

where the base rates π_k were equally and uniformly selected as $\pi_k = \frac{1}{K}$ to represent equal prior probabilities associated with labels due to the ease of deployment and equal importance/priority among labels. The Dirichlet distribution is a Probability Density Function

(PDF) for possible labels of the latent categorical distribution \mathbf{c} that is denoted by $Dir(\mathbf{c}|\boldsymbol{\alpha})$. This PDF is used as the conjugate prior distribution for the categorical distribution \mathbf{c} since the posterior distribution after incorporating the knowledge gained from the observed data, is also a Dirichlet distribution. The Dirichlet distribution PDF $Dir(\mathbf{c}|\boldsymbol{\alpha})$ is characterized by the parameter set $\boldsymbol{\alpha}$ as,

$$Dir(\mathbf{c}|\boldsymbol{\alpha}) = \begin{cases} \frac{1}{B(\boldsymbol{\alpha})} \prod_{i=1}^K c_i^{\alpha_i-1} & \text{for } \mathbf{c} \in \mathcal{V}_K \\ 0 & \text{otherwise} \end{cases},$$

where $B(\boldsymbol{\alpha})$ is the K -dimensional multivariate beta function (Kotz et al., 2019), and \mathcal{V}_K is the $(K - 1)$ -dimensional unit simplex such that

$$\mathcal{V}_K = \{\mathbf{c} \mid \sum_{i=1}^K c_i = 1 \quad \text{and} \quad 0 \leq c_1, c_2, \dots, c_K \leq 1\}.$$

Therefore, the Dirichlet parameter set $\boldsymbol{\alpha}$ is considered over all possible outcomes in classifying any given data sample. When a data sample is observed by the model, the sample is linked to one of the K labels and the corresponding Dirichlet parameter α_k is increased, e.g., due to identifying a specific pattern within an image. Then, the Dirichlet distribution is updated based on the new observation. The expected probability of the Dirichlet distribution, projected by each target label, is considered as the predictive probability $p_k \in \mathbf{P}$ associated with the label k , and computed as,

$$\mathbb{E}_{Dir(\mathbf{c}|\boldsymbol{\alpha})}[c_k \in \mathbf{c}] = p_k = \frac{\alpha_k}{\alpha_0}, \quad \text{where} \quad \alpha_0 = \sum_{k=1}^K \alpha_k = K + \sum_{k=1}^K e_k. \quad (2)$$

The summation of Dirichlet parameters denoted by α_0 is called Dirichlet strength, indicating the total collected evidence in classifying a data point. Using the Dirichlet distribution $\boldsymbol{\alpha}$, the belief masses b_k indicating the confidence associated with the label k , and the *uncertainty* of the model (epistemic) are computed as,

$$b_k = \frac{e_k}{\alpha_0} \quad \text{and} \quad u = \frac{K}{\alpha_0} \quad \text{s.t.} \quad u + \sum_{k=1}^K b_k = 1, \quad (3)$$

where $0 \leq b_k < 1$ denotes belief masses that are directly correlated with the evidence e_k associated with the label k and they are sub-additive to 1 (i.e. the summation of belief masses are less than 1). The model uncertainty $0 < u \leq 1$ is considered as our heuristic notion of uncertainty and defined as follows:

Definition 3 (Heuristic Model Uncertainty) *A complete lack of confidence over all target labels in a DNN classifier is called the model (epistemic) uncertainty over all possible model outcomes that is heuristically used to devise a non-conformity score function in CP.*

The model uncertainty u is inversely proportional to the total collected evidence for supporting the target labels. In CP, a non-conformity score function is devised based on a heuristic notion of model uncertainty. In our non-conformity score function, the model uncertainty u obtained from evidential setting carries heuristic notion of uncertainty.

3.2. Evidential Classification Cost

In CP, when we construct prediction sets, three distinct properties are required to be satisfied. The first property is the *marginal coverage* or validity that guarantees to include the true label in the prediction sets based on the following theorem (Vovk et al., 2005):

Theorem 4 (Conformal Coverage Guarantee) *Consider \mathcal{X}_{cal} and $(x_{val}, y_{val}) \in \mathcal{X}_{val}$ are i.i.d. and correspond to unseen test data as holdout data and a validation data point, respectively. Let δ be the user-chosen coverage error level, \hat{q} is the $1 - \delta$ quantile of holdout non-conformity scores, and $\mathcal{C} : \mathbb{R}^d \times \mathbb{R} \rightarrow 2^{\mathcal{Y}}$ be the set-valued predictor function for all possible labels in \mathcal{Y} . Then, the probability of the true label being covered in the prediction set is guaranteed as follows:*

$$\mathcal{P}(y_{val} \in \mathcal{C}(x_{val}, \hat{q})) \geq 1 - \delta . \tag{4}$$

The second property is the *set size* or efficiency to reflect the desirability of a smaller size for the prediction set. The third property is the *adaptivity* that necessitates the set size for unseen data is modified to represent instance-wise model uncertainty, i.e., the set size is smaller when the model encounters easier test data rather than the inherently harder ones. Note that the difficulty of a test data point is based on the rank of its true label in the sorted set of outcome probabilities. These properties affect each other; for example, the set size property tries to make the sets smaller, while the adaptivity property tries to make the sets larger for harder data points when the model is uncertain. Similarly, choosing sets with a fixed size may satisfy the coverage property, but without adaptivity.

In multi-class classification tasks, a DNN classifies a data point to a specific target label; the one with the highest predictive probability. In this process, not all unselected target labels for the given data point are equivalent as each one of them may carry a different predictive probability, albeit the probability is lower than the probability of the selected target label. We use this notion along with other evidential properties to define *Evidential Classification Cost (ECC)* for each label $k \in \mathcal{Y}$ as follows:

Definition 5 (Evidential Classification Cost) *The amount of cost or error that a pre-trained classifier indicates based on evidential properties when classifying a data point into a specific target label.*

In other words, ECC represents an estimation of how much each target label $k \in \mathcal{Y}$ is not a correct choice to classify a particular data point. The evidential properties are used as additional information to support not only for the true label, but also for all other labels in each prediction. Thus, a model produce the lowest value (minimum) of ECC for the true label when correctly classifying a data point. We use two evidential properties *Uncertainty Surprisal* and *Expected Utility* to subjectively quantify ECC associated with each target label leading to computing our non-conformity score function. We call this cost subjective as it reflects the notion that these two properties are carried and affected by each one of the target labels individually. ECC is different and computationally independent from the objective cost computed by the model’s loss function (objective function).

According to Equations (2) and (3), the model uncertainty u is achieved by considering the beliefs associated with all the target labels when classifying a data point. The portion of the uncertainty u associated with each label k is called *Focal Uncertainty* U_k that is partitioned based on the corresponding prior probability π_k as,

$$U_k = u\pi_k . \tag{5}$$

As we obtain the focal uncertainty associated with each label, we can now measure the first evidential property called uncertainty surprisal that is defined in information theory as follows (Jøsang, 2016):

Definition 6 (Uncertainty Surprisal) *The uncertainty surprisal distribution I_U over target labels is the amount of information required to confidently predict the model outcomes based on its corresponding predictive probability distribution.*

In EDL, the predictive probability p_k is considered as the projected probability for the target label $k \in \{1, 2, \dots, K\}$ when the pretrained model \mathcal{M} is tested with each data point. The surprisal of the target label k is then computed by the negative logarithm of the predictive probability p_k as,

$$I(k) = -\log p_k . \tag{6}$$

The surprisal function, $I(k)$, measures the degree of an outcome is surprising. High surprisal shows that we require more information to predict the outcome, whereas low surprisal shows that we require less information to predict the outcome. Therefore, the uncertainty is directly intertwined with the surprisal such that the more surprisal associated with a target label, the more uncertainty we encounter in selecting the label to classify an input data point. To avoid misclassification and maintain the performance, we expect the model to have low surprisal on a specific target label. As we aim to produce adaptive non-conformity scores for target labels of each data point, we exploit a particular surprisal function based on the focal uncertainty associated with each target label. This surprisal function is called *Focal Uncertainty Surprisal* which is denoted by $I_U(k)$ for a data point and defined as,

$$I_U(k) = \frac{U_k I(k)}{p_k} , \tag{7}$$

where p_k is the predictive probability, $I(k)$ is the surprisal function, and U_k is the focal uncertainty associated with the label k . Note that as shown in Equation (5), the model uncertainty u and the base rate π_k (i.e., prior probability) of the label k are taken into account to compute focal uncertainty U_k . Now, we define the second evidential property called expected utility as follows (Jøsang, 2016):

Definition 7 (Expected Utility) *Considering the predictive probability distribution \mathbf{P} over possible model outcomes, an expected utility distribution Φ over target labels is a distribution expressing the expected performance or effectiveness of a learning model associated with the model outcome distribution.*

In a learning model, we compute the expected utility distribution associated with target labels by the element-wise product of φ over target labels and the corresponding predictive

probability distribution \mathbf{P} obtained by Dirichlet parameters. Specifically, the expected utility $\Phi(k)$ of the model \mathcal{M}_Θ when classifying a data point to the label k is defined as,

$$\Phi(k) = \phi_k p_k, \quad (8)$$

where $\phi_k \in \boldsymbol{\varphi}$ and $p_k \in \mathbf{P}$ denote the utility and the predictive probability associated with the target label k when a data point is classified. Since softmax probabilities can represent the performance of a learning model when classifying a data point into a target label, we apply softmax function $\sigma(\cdot)$ to the K logits and consider it as the corresponding utility distribution $\boldsymbol{\varphi}$ when classifying the data point $x \in \mathcal{X}$ such that $\boldsymbol{\varphi} = \sigma(\mathcal{M}(x))$. Note that it is also possible to consider other aspects of the model performance or effectiveness as the utility distribution associated with the model outcomes.

3.3. Evidential Prediction Set

For a pretrained model, we use *split conformal prediction* in which we split all the available test (unseen) data \mathcal{X} into holdout (calibration) data \mathcal{X}_{cal} and validation data \mathcal{X}_{val} such that $\mathcal{X} = \mathcal{X}_{cal} \cup \mathcal{X}_{val}$ and $\mathcal{X}_{cal} \cap \mathcal{X}_{val} = \emptyset$. When classifying an unseen data point (e.g., an image), the difficulty level of the data point denoted by r_y is defined as the rank of its true label $y \in \mathcal{Y}$ in the descending-sorted set of predictive probabilities from the highest to lowest values denoted by $\langle p_k \rangle$ (Angelopoulos et al., 2020). This difficulty level can be incorporated in ECC and non-conformity score since the prediction sets should be larger for more difficult images that has higher true label rank rather than the easier ones due to adaptivity criterion. Therefore, in classifying a data point, when the rank of label k denoted by $r_k \in \{0, 1, \dots, K - 1\}$ in a descending-sorted set of predictive probabilities $\langle \mathbf{P} \rangle$ is higher, the ECC associated with the label k is also increased. We define the scaling function $\rho(k)$ to quantify the impact of r_k on ECC as,

$$\rho(k) = \frac{K}{K - r_k}, \quad (9)$$

where K is the constant number of possible target labels and r_k is the rank of label k in descending-sorted set of predictive probabilities. To incorporate r_k in ECC, we require $\rho(k)$ to scale r_k and suppress its extent. Note that $\rho(k)$ is an increasing function with respect to increasing r_k . Furthermore, when $r_k = 0$ (i.e., first rank), $\rho(k)$ has no impact on ECC, the label k is the most probable label and have the highest predictive probability as $p_k = \max_{\nu \in \mathcal{Y}} p_\nu$.

We denote ECC associated with the label k as C_k that is dependent on the two evidential properties (i.e., uncertainty surprisal and expected utility) and the rank associated with the target labels. Following the interpretations of focal uncertainty surprisal in Equation (7) and expected utility in Equation (8), ECC is directly proportional to the focal uncertainty surprisal as $C_k \propto I_U(k)$, and inversely proportional to the expected utility as $C_k \propto \frac{1}{\Phi(k)}$. Lower predictive probability p_k gives rise to higher focal uncertainty surprisal $I_U(k)$, lower expected utility $\Phi(k)$, higher entropy, higher model uncertainty u , and ultimately, higher C_k for label k in classifying a data point. According to Equation (9), ECC is also directly proportional to the label rank r_k and its scaling function $\rho(k)$ as $C_k \propto \rho(k)$ since higher

rank for label k implies lower p_k that gives rise to higher C_k . Using Equation (9), the difficulty of a data point, i.e. true label rank, can contribute to both the proposed C_k and non-conformity score $S_{ECC}(k)$. Thus, we define evidential classification cost C_k associated with classifying a data point into the target label k as,

$$\begin{aligned}
 C_k &= \frac{\rho(k)I_U(k)}{\Phi(k)} = Ku \overbrace{\frac{-\pi_k \log p_k}{\phi_k p_k^2 (K - r_k)}}^{\widehat{C}_k} \\
 \implies C_k &= Ku \widehat{C}_k \quad \text{such that} \quad \widehat{C}_k = -\frac{\pi_k \log p_k}{\phi_k p_k^2 (K - r_k)},
 \end{aligned} \tag{10}$$

where K is the number of possible labels, u denotes the model uncertainty, p_k denotes the predictive probability, π_k denotes the base rate, r_k denotes the rank of the label k 's probability. $\phi_k = \sigma_k(\mathcal{M}(x))$ denotes the utility function associated with the data point $x \in \mathcal{X}$ and the target label k in the model \mathcal{M} which is considered as the softmax probability of the label k (note that $\sigma(\cdot)$ is the softmax function). We also call the term \widehat{C}_k in Equation (10) as *Label Evidential Cost*, which is completely dependent on the label k . Then, for each data point $x \in \mathcal{X}$, we normalize (scale) C_k to define the proposed evidential non-conformity score $S_{ECC}(k)$ associated with label k that is computed as,

$$\forall k \in \mathcal{Y}: \quad S_{ECC}(k) = \frac{C_k}{\max_{\nu \in \mathcal{Y}} C_\nu}, \tag{11}$$

where C_k is ECC associated with the label $k \in \mathcal{Y}$ for a single data point.

To construct our evidential prediction set $\mathcal{C}(x_{val}, \widehat{q})$ for an unseen data point $x_{val} \in \mathcal{X}_{val}$, we first apply the proposed evidential non-conformity score $S_{ECC}(k)$ defined in Equation (11) to the data in holdout set \mathcal{X}_{cal} that is uniformly and randomly partitioned from testing dataset such that $|\mathcal{X}_{cal}| = n$. Then, for each holdout data point, we order the evidential scores $S_{ECC}(k)$ for all $k \in \mathcal{Y}$ based on the descending-sorted set of their predictive probabilities $\langle p_k \rangle$, i.e. evidential scores associated with labels having the highest to the lowest predictive probabilities. We can now select the evidential non-conformity score $S_{ECC}(k = r_y)$ associated with the rank of the true label $y \in \mathcal{Y}$ in the descending-sorted set of predictive probabilities. Once we have n holdout evidential scores corresponding to holdout data, we quantify the $(1 - \delta)$ -quantile of these scores as \widehat{q} . The quantile \widehat{q} acts as a threshold that determines for each unseen data point, which one of the labels should be included in the prediction set \mathcal{C} . Finally, for each unseen data point $x_{val} \in \mathcal{X}_{val}$, we calculate $S_{ECC}(k)$ in Equation (11) for all the labels $k \in \mathcal{Y}$ exactly as the same procedure we had for holdout data, and include each label k that meets the following inequality in the prediction set $\mathcal{C}(x_{val}, \widehat{q})$:

$$\mathcal{C}(x_{val}, \widehat{q}) = \{ k \in \mathcal{Y} \mid S_{ECC}(k) \leq \widehat{q} \}, \tag{12}$$

where \widehat{q} is $(1 - \delta)$ -quantile of the evidential non-conformity scores $S_{ECC}(k = r_y)$ associated with the true label rank r_y of holdout data \mathcal{X}_{cal} .

3.4. Insights on Evidential Conformal Prediction

According to evidential non-conformity score $S_{ECC}(k)$ associated with labels $k \in \mathcal{Y}$ introduced in Equation (11), we have several insights that shows ECP is a promising method in producing prediction sets in CP: (1) When the predictive probability p_k is decreased due to misclassification or out-of-distribution input data, C_k is increased significantly due to the different components containing p_k in Equation (10) and consequently, $S_{ECC}(k)$ will be increased which represents higher uncertainty and worse fit between x and the label k . (2) Based on Equation (3), as more evidence is collected when classifying a data point, i.e. $\sum_{k=1}^K e_k$, the model uncertainty u associated with all the labels is decreased that yields to decreasing C_k and $S_{ECC}(k)$ for the label k . Therefore, the model uncertainty u in Equation (10) acts as a coefficient to further adapt the non-conformity score with the input data, particularly when the model encounters an input far from the training distribution. (3) In Equation (10), the base rate or prior probability π_k contributes to computing C_k (ECC) associated with the target label k . Since changing the base rate of each target label can lead to a change in the C_k of the target label, prior probabilities are incorporated in the ECC which can be considered as a parameter to consider fairness or balance class frequency among possible classes in the proposed non-conformity score function. (4) The choice of utility function is not limited to the softmax function. A modeller can consider other measurements or functions to produce utility distribution φ associated with labels, but with respect to the correlation and inverse proportionality between $\Phi(k)$ and C_k . (5) Using evidential setting, we can measure the reliability of marginal coverage by computing the uncertainty and confidence associated with coverage as described in the next section.

3.5. Reliability in Marginal Coverage

According to stochasticity and randomness in sampling the holdout set with size $|\mathcal{X}_{cal}| = n$ in CP, different trials on infinite number of validation data indicate different marginal coverage in prediction sets. Based on Equation (4), the marginal coverage is at least $1 - \delta$ over this random sampling of holdout set. However, for a fixed holdout set, the marginal coverage on infinite validation data is not exactly $1 - \delta$. To restrict the deviations from $1 - \delta$ in the marginal coverage, we require to use holdout set with adequately large n while having the coverage distribution (Angelopoulos et al., 2023). Formally, the distribution of coverage given a fixed holdouts set follows a Beta distribution (Vovk, 2012) based on the size of holdout set n as,

$$\begin{aligned} \mathcal{P}(y_{val} \in \mathcal{C}(X = x_{val}) \mid \mathcal{X}_{cal}) &\equiv \mathbb{E}[y_{val} \in \mathcal{C}(X = x_{val}) \mid \mathcal{X}_{cal}] \sim \text{Beta}(n + 1 - l, l) \\ \text{s.t.} \quad l &= \lfloor (n + 1)\delta \rfloor, \end{aligned} \quad (13)$$

where $n = |\mathcal{X}_{cal}|$ denotes the size of holdout set, and δ denotes the coverage error level. This conditional expectation on fixed holdout data represents the coverage associated with a large set of validation data (infinite validation data in its perfect form).

Following Theorem 4, consider δ as the error level of true label coverage, $|\mathcal{X}_{cal}| = n$ is the size of holdout set, and $\mathcal{C} : \mathbb{R}^d \rightarrow 2^{\mathcal{Y}}$ as the prediction set function for unseen validation data $x_{val} \in \mathcal{X}_{val}$ with the true label y_{val} . As the coverage distribution is conditional on a fixed holdout set, the uncertainty in coverage and the confidence associated with correctly covering the true label is highly dependent on n . We propose the following theorem to

quantify the confidence and uncertainty associated with true label coverage as the reliability measures:

Theorem 8 (Coverage Confidence Guarantee) *Suppose \mathcal{Y} be the set of target labels, \mathcal{X}_{cal} be the holdout set with size n , and $\mathcal{C} : \mathbb{R}^d \rightarrow 2^{\mathcal{Y}}$ be the set-valued predictor with the coverage error level δ . If for infinite number of validation data \mathcal{X}_{val} , the expected true label coverage of \mathcal{C} is conditional on a fixed holdouts set \mathcal{X}_{cal} , then $\mathcal{C}(x_{val} \in \mathcal{X}_{val})$ is γ -confident in coverage such that:*

$$\gamma = \frac{n - \lfloor (n+1)\delta \rfloor}{n+1} \quad \text{where} \quad \frac{n}{n+1} - \delta \leq \gamma < 1 - \delta, \quad (14)$$

and the uncertainty $U_{\mathcal{C}}$ in the expected coverage of \mathcal{C} is computed as,

$$U_{\mathcal{C}} = \frac{2}{n+1}. \quad (15)$$

The proof of Theorem 8 is provided in Appendix A. This theorem indicates that with a large number of validation data, the expected coverage of true labels in prediction sets given a fixed set of holdout set is associated with an amount of uncertainty $U_{\mathcal{C}}$. Thus, we consider γ degree of confidence in covering the true labels in prediction sets. A modeller can quantify the reliability in conformal coverage using these two measures. In the following section, we elaborate on our practical experiments in detail and demonstrate the evaluation results for the proposed method compared to the SoTA CP methods in producing prediction sets.

4. Experimental Evaluations

In this section, we report our experiments on the validity (true label coverage), efficiency (set size), and adaptivity for the produced prediction sets of our approach *ECP* compared to two state-of-the-art (SoTA) conformal approaches, *APS* (Romano et al., 2020), and *RAPS* (Angelopoulos et al., 2020), along with a baseline approach as *Base* method. The *Base* approach directly utilizes softmax probabilities to include all predicted labels from the most likely to the least likely in the prediction set until their cumulative probabilities exceeds a user-specified probability threshold. Note that in *Base* approach, true label coverage may not be guaranteed.

Model Architectures and Datasets. For fair comparative evaluations with SoTA methods, we are using nine pretrained image classifiers: ResNet (He et al., 2016), VGG (Simonyan and Zisserman, 2014), DenseNet (Huang et al., 2017), ShuffleNet (Ma et al., 2018), Inception (Szegedy et al., 2016), and ResNeXT (Xie et al., 2017) from Pytorch framework with standard hyperparameters. We also used two different test sets of ImageNet with 1000 class labels *ImageNet-Val* (with 50K test images) and *ImageNet-V2* (with 10K test images) after standard transformations and normalization.

Experimental Setup. We implemented our method in Python using PyTorch framework¹, and the assessments have been performed on a machine with Intel(R) Core(TM)

1. The source codes of the experiments are available at: <https://github.com/tailabTMU/ECP>

i7-10750H 2.60GHz (6 cores) processor, NVIDIA Tesla T4 GPU, and 32GB RAM allocated to our computation. We apply temperature scaling (Guo et al., 2017) for Base, APS, and RAPS methods using holdout data to find the optimal temperature for calibrating softmax scores before using them as predictive probabilities. In our experiments, we use 15K and 3K of data as holdout set to calibrate and quantify the $(1 - \delta)$ -quantile \hat{q} of non-conformity scores for ImageNet-Val and ImageNet-V2, respectively. We evaluate RAPS using its regularization hyperparameters $k_{reg} = 5$ and different choices of constant penalty called $\lambda = \{0.0001, 0.001, 0.01, 0.1, 1\}$ that were introduced to encourage small set sizes by skipping the first k_{reg} highest probable labels ($0 \leq k_{reg} \leq K$) and then, penalizing the other softmax scores by a fixed $0 < \lambda \leq 1$. Note that since RAPS is the regularized version of APS, we represent APS by setting $\lambda = 0$ in RAPS. We conduct four sets of experimental evaluations as reported in the forthcoming subsections. Note that all results are averaged over different trials, and the negligible discrepancies between the empirically reported and theoretically guaranteed (Theorem 4) coverage results are due to stochasticity and randomness in finite number of trials.

4.1. Experiment 1: Marginal Coverage and Prediction Set Size

In this experiment, we calculate the average marginal coverage and set size of our method and each of the other three SoTA methods for two different choices of coverage error levels $\delta = 0.1$ reported in Table 1 and $\delta = 0.05$ reported in Appendix B over 10 different trials. We use both ImageNet-Val and ImageNet-V2 test data, and in each trial, we randomly split the test data into two subsets as 30% of holdout set (calibration set) and 70% of validation set. We report the mean over trials for average marginal coverage and set size for ImageNet-Val and ImageNet-V2 in Tables 1 and 2, respectively. We also plot the results of ResNet-152 model as our base classifier on ImageNet-Val to compare the performance of our method with the other CP methods when choosing different coverage error level in Figure 2. Unlike RAPS, ECP does not require any hyperparameters to be fine-tuned for a specific purpose which may cause computational burden. Therefore, we use $k_{reg} = 5$ and $\lambda = 0.1$ in these experiments as benchmark reported in (Angelopoulos et al., 2020) to apply RAPS method.

Observations. We observe that our method (ECP) outperforms other methods in terms of prediction set size (last column) while choosing different coverage levels $1 - \delta$ in Figure 2(a). Furthermore, as shown in Figure 2(b), ECP guarantees the marginal coverage with different δ as same as SoTA methods except Base approach due to the noise in tail softmax probabilities. Based on the results reported in Tables 1 and 2, for each model architecture, ECP (the boldfaced column) has always smaller prediction sets on average for both test datasets compared to Base, APS, and RAPS, while guaranteeing the marginal coverage of true labels as $1 - \delta$ in the produced prediction sets. Note that regardless of how hyperparameters are chosen in RAPS (even if RAPS is optimized to have small sets), ECP outperforms RAPS in terms of efficiency by producing smaller and more precise prediction sets. Moreover, the variance (fluctuations) in marginal coverage is higher when testing on ImageNet-V2 due to having less data and different distribution compared to training data. Nevertheless, ECP is also able to produce smaller sets and still guarantee marginal coverage when tested on ImageNet-V2 if holdout set is selected from the new distribution. We observe a similar behaviour when $\delta = 0.05$. We report the results for $\delta = 0.05$ in Appendix B to highlight

Table 1: Efficiency on **ImageNet-Val**: The median-of-means for marginal coverage and prediction set size using different architectures and methods with $\delta = 0.1$ over 10 trials.

Model	Performance	Mean Marginal Coverage				Mean Prediction Set Size			
	Accuracy	Base	APS	RAPS	ECP	Base	APS	RAPS	ECP (Ours)
ResNeXT101	79.31%	0.887	0.900	0.900	0.900	17.76	20.62	2.63	1.64
ResNet152	78.31%	0.893	0.901	0.900	0.900	9.64	10.36	2.67	1.75
ResNet101	77.37%	0.897	0.900	0.900	0.900	10.19	10.81	2.75	1.85
ResNet50	76.13%	0.895	0.900	0.900	0.901	11.64	12.93	3.05	2.04
ResNet18	69.76%	0.896	0.900	0.899	0.900	15.60	16.53	4.38	3.72
DenseNet161	77.13%	0.892	0.901	0.899	0.901	11.71	12.82	2.83	1.82
VGG16	71.59%	0.895	0.901	0.901	0.900	13.81	14.16	3.70	2.97
ShuffleNet	69.36%	0.896	0.901	0.900	0.899	29.33	32.40	4.56	3.98
Inception	69.54%	0.886	0.901	0.900	0.900	76.00	89.84	4.99	4.18

Table 2: Efficiency on **ImageNet-V2**: The median-of-means for marginal coverage and prediction set size using different architectures and methods with $\delta = 0.1$ over 10 trials.

Model	Performance	Mean Marginal Coverage				Mean Prediction Set Size			
	Accuracy	Base	APS	RAPS	ECP	Base	APS	RAPS	ECP (Ours)
ResNeXT101	67.51%	0.891	0.901	0.900	0.900	35.32	54.67	5.56	4.88
ResNet152	66.98%	0.895	0.900	0.900	0.900	25.11	29.67	5.52	4.28
ResNet101	65.54%	0.893	0.900	0.899	0.899	29.06	33.34	8.66	5.65
ResNet50	63.20%	0.884	0.899	0.901	0.900	31.46	33.53	9.34	6.68
ResNet18	57.29%	0.896	0.900	0.900	0.901	38.85	40.03	17.71	11.68
DenseNet161	65.13%	0.891	0.900	0.900	0.900	28.18	32.14	6.42	5.72
VGG16	58.81%	0.881	0.899	0.898	0.900	31.56	32.91	13.85	9.74
ShuffleNet	56.04%	0.885	0.901	0.900	0.899	66.40	75.84	24.99	17.90
Inception	57.59%	0.891	0.900	0.900	0.900	132.75	158.49	16.77	15.09

that our proposed method is compatible with higher guarantees of marginal coverage and its ability to produce smaller sets compared to SoTA methods. Note that in both test sets, we use significantly smaller holdout set to quantify the quantile compared to the results already reported in RAPS method (Angelopoulos et al., 2020). This shows the strength of ECP that even with limited holdout data, ECP outperforms SoTA methods in terms of efficiency, i.e. achieving smaller and more precise prediction sets.

4.2. Experiment 2: Coverage in Size-stratified Prediction Sets

In this experiment, we stratify the size of the prediction set produced by our method and the other three SoTA methods into different ranges $\{0 - 1, 2 - 3, 4 - 6, 7 - 10,$

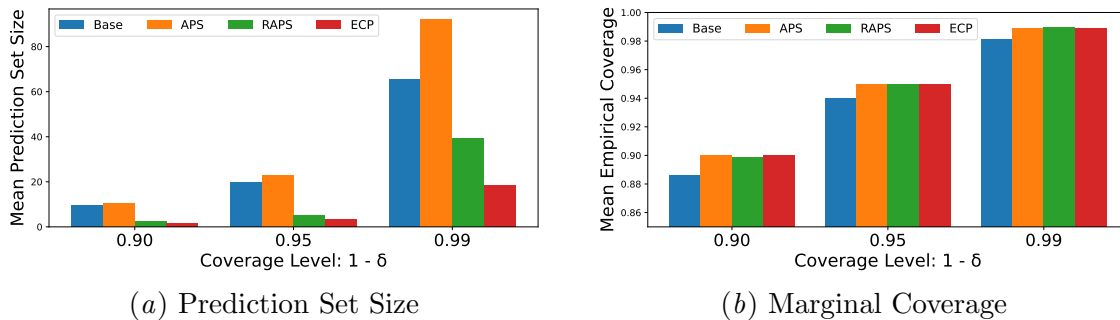


Figure 2: Comparing ECP with SoTA methods using ResNet-152 with different choices of $\delta = \{0.1, 0.05, 0.01\}$ in terms of the average marginal coverage and prediction set size. For RAPS, we used $k_{reg} = 5$ and $\lambda = 0.1$.

Table 3: The count and average coverage of images stratified by their prediction set sizes on ImageNet-Val using ResNet-152 with $\delta = 0.1$ and different λ to evaluate APS and RAPS.

Set Size	ECP (Ours)		APS ($\lambda = 0$)		$\lambda = 0.001$		$\lambda = 0.01$		$\lambda = 0.1$		$\lambda = 1$	
	cnt	cvg	cnt	cvg	cnt	cvg	cnt	cvg	cnt	cvg	cnt	cvg
0 to 1	18322	0.932	20149	0.880	20177	0.879	19416	0.894	18422	0.910	17521	0.927
2 to 3	13981	0.874	6524	0.910	6418	0.913	6643	0.923	6764	0.928	6824	0.941
4 to 6	2639	0.833	2196	0.913	2313	0.922	2885	0.929	6540	0.904	10655	0.833
7 to 10	58	0.880	1242	0.927	1313	0.923	2259	0.915	3170	0.758	0	-
11 to 100	0	-	3873	0.951	4583	0.938	3797	0.875	104	0.471	0	-
101 to 1000	0	-	1016	0.972	196	0.903	0	-	0	-	0	-

11 – 100, 101 – 1000} to evaluate the coverage of prediction sets in each size range. We use ResNet-152 on ImageNet-Val with the coverage error level $\delta = 0.1$ and different choices of hyperparameters λ for RAPS.

Observations. In Table 3, we observe that APS covers true labels in prediction sets of sizes 101 – 1000 with a high probability around 97% that is much higher than the desired coverage 90%, i.e., APS aims to guarantee marginal coverage by undercovering easy examples (smaller set sizes) and overcovering difficult examples (larger set sizes) which is not an acceptable behavior since APS is far from the *exact conditional coverage*. Note that the exact conditional coverage is defined for a specific test data point (conditionality) as $\mathcal{P}(y_{val} \in \mathcal{C}(X, \hat{q}) \mid X = x_{val}) = 1 - \delta$. For RAPS, when λ is small, RAPS produces larger sets. However, when λ is high, RAPS produces smaller sets (at most with the size k_{reg}), but with less stability in conditional coverage since as shown in Table 3, with high λ , the coverage of RAPS for larger set sizes are farther from exact conditional coverage, i.e. $1 - \delta$, compared to ECP. Thus, ECP is more likely to have or to be near exact conditional coverage rather than RAPS when produces smaller sets with high λ although ECP always produces smaller sets rather than RAPS even in these cases. Note that RAPS with light regularization (lower λ) is stable and more balanced compared to when λ is high.

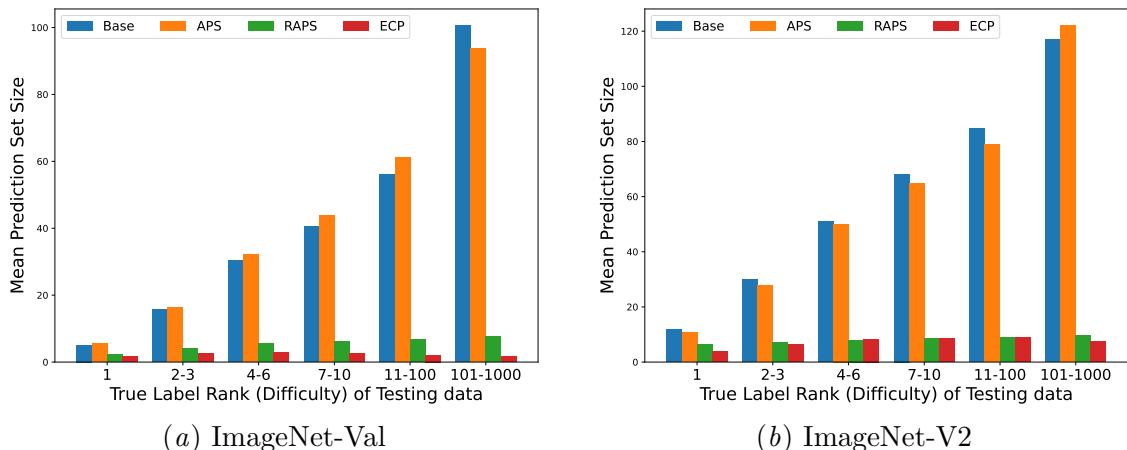


Figure 3: Adaptivity in ECP compared to SoTA methods based on difficulty level for both test datasets using ResNet-152 with $\delta = 0.1$. For RAPS, we used $k_{reg} = 5$ and $\lambda = 0.1$.

4.3. Experiment 3: Adaptivity in Prediction Sets

In this section, we address the adaptivity criterion to evaluate our method compared to the other methods based on difficulty level of test images. The difficulty of an image is determined and represented by the rank of the true label’s predictive probability in the descending-sorted set of predictive probabilities associated with the target labels. Table 4 shows the average marginal coverage and set size for the methods based on different ranges of difficulty level in test data. We stratify the image difficulty levels into different ranges $\{1, 2 - 3, 4 - 6, 7 - 10, 11 - 100, 101 - 1000\}$ to evaluate and compare the adaptivity of the methods in each difficulty range. Moreover, Figure 3 shows the average set size for the methods based on different difficulty ranges for both ImageNet-Val (Figure 3(a)) and ImageNet-V2 (Figure 3(b)).

Observations. The results show that ECP produces smaller prediction sets for easy images (low difficulty levels) compared to the difficult ones. We observe that ECP maintain its adaptivity while producing smaller set sizes on average rather than other SoTA methods when testing with both datasets. Because of trade-off between adaptiveness and set size, ECP aims to produce the smallest possible sets for difficult images (even empty sets) where there is no significant or useful coverage in prediction sets as shown in Table 4. We can see the poor coverage for both ECP and RAPS methods in predicting difficult images due to producing small sets compared to APS method. Thus, ECP uses this phenomenon to further reduce the set sizes for difficult images, even with producing more empty sets, while their sizes are significantly larger than easy images to preserve adaptivity. Although ECP and RAPS (with high λ) both cover difficult images less than $1 - \delta$ to produce smaller sets, ECP compensates it by carefully having slightly larger sets for easy images which leads to higher coverage compared to RAPS to guarantee $1 - \delta$ marginal coverage on average. Note that this increase in set size for easy images is adequately slight due to the higher number of easy images rather than difficult ones.

Table 4: The average marginal coverage and set size of images stratified by their difficulty levels, i.e. the rank of true label’s predictive probability, on ImageNet-Val using ResNet-152 with $\delta = 0.1$ and different λ to evaluate APS and RAPS.

Difficulty	ECP (Ours)			APS/RAPS			$\lambda = 0.01$		$\lambda = 0.1$		$\lambda = 1$	
	cnt	cvg	sz	cnt	cvg	sz	cvg	sz	cvg	sz	cvg	sz
1	27336	0.999	1.47	27428	0.951	5.44	0.959	2.60	0.970	2.07	0.977	2.02
2 to 3	4573	0.817	2.56	4524	0.783	16.19	0.810	6.27	0.830	4.04	0.866	3.64
4 to 6	1239	0.203	2.84	1229	0.695	32.32	0.726	9.97	0.727	5.49	0.659	4.57
7 to 10	621	0.005	2.64	598	0.640	41.53	0.624	11.97	0.247	5.89	0	4.61
11 to 100	1092	0	2.32	1085	0.562	60.02	0.281	15.52	0	6.65	0	4.88
101 to 1000	139	0	2.00	136	0.220	101.42	0	20.95	0	7.33	0	5.02

Table 5: The quality of prediction sets of ImageNet-Val data based on the average of size-adaptivity trade-off (SAT) score with respect to average set size and SSCV in different methods and model architectures with $\delta = 0.1$.

Model	APS			RAPS			ECP (Ours)		
	Size	SSCV	SAT	Size	SSCV	SAT	Size	SSCV	SAT
ResNeXT101	19.21	0.088	0.045	4.43	0.029	0.212	1.68	0.061	0.551
ResNet152	10.85	0.072	0.082	3.93	0.025	0.239	1.77	0.077	0.517
ResNet101	11.01	0.071	0.081	4.21	0.024	0.224	1.85	0.076	0.481
ResNet50	12.59	0.069	0.071	4.54	0.029	0.207	2.03	0.080	0.411
ResNet18	16.44	0.050	0.056	5.43	0.002	0.183	3.68	0.075	0.236
DenseNet161	11.82	0.077	0.075	4.17	0.020	0.227	1.85	0.070	0.470
VGG16	14.06	0.049	0.065	8.92	0.016	0.107	2.97	0.067	0.292
ShuffleNet	31.24	0.059	0.029	6.31	0.001	0.158	4.01	0.128	0.227
Inception	87.87	0.084	0.010	5.87	0.002	0.169	4.15	0.132	0.241

4.4. Experiment 4: Adaptivity in Conditional Coverage

In this experiment, we evaluate ECP compared to other methods based on the adaptivity in conditional coverage which is considered a promising approach to assess adaptiveness in image classifiers (Angelopoulos et al., 2020). A set predictor function $\mathcal{C} : \mathbb{R}^d \rightarrow 2^{\mathcal{Y}}$ satisfies exact conditional coverage for each $x_{val} \in \mathcal{X}_{val}$ if $\mathcal{P}(y \in \mathcal{C}(X) \mid X = x_{val}) = 1 - \delta$. Practically, this exact conditional coverage is infeasible in distribution-free setting, i.e. guaranteeing exact conditional coverage requires distributional assumptions on input data (Vovk, 2012), but it can be satisfied approximately. Furthermore, exact conditional coverage requires a perfect classifier (i.e., trained on infinite data) with high accuracy, and cannot be achievable in real world due to limited and realistic sample sizes during training.

Alternatively, RAPS followed the notion of local conditional coverage (Tibshirani et al., 2019) where the coverage in a neighborhood of each unseen data point is considered and weighted based on the size of the neighborhood. Therefore, if exact conditional coverage holds, then it holds for size-stratified prediction sets (Angelopoulos et al., 2020). Formally, if $\mathcal{P}(y \in \mathcal{C}(X) \mid X = x_{val}) = 1 - \delta$, then $\mathcal{P}(y \in \mathcal{C}(X) \mid |\mathcal{C}(X)| \in \mathcal{S}) = 1 - \delta$ for any $\mathcal{S} \subset \{0, 1, 2, \dots, K\}$ where $K = |\mathcal{Y}|$ is the number of labels and \mathcal{S} is a subset of different sizes for prediction sets. In practice, a relaxation is considered for coverage of size-stratified sets as $\mathcal{P}(y \in \mathcal{C}(X) \mid |\mathcal{C}(X)| \in \mathcal{S}) \geq 1 - \delta$ for any $\mathcal{S} \subset \{0, 1, 2, \dots, K\}$.

A measure of adaptivity in prediction sets is introduced in (Angelopoulos et al., 2020) as *Size-stratified Coverage Violation (SSCV)*, which is based on the violations from size-stratified conditional coverage. Consider $\mathcal{S}_i \subset \{0, 1, 2, \dots, K\}$ are disjoint set-size ranges such that $\bigcup_{i=1}^{i=s} \mathcal{S}_i = \{0, 1, 2, \dots, K\}$, and \mathcal{I}_i is the set of data indices j that their prediction set sizes are in set-size range \mathcal{S}_i such that $\mathcal{I}_i = \{j : |\mathcal{C}(X_j)| \in \mathcal{S}_i\}$. Then, the metric SSCV for the set-valued predictor \mathcal{C} and set-size ranges $\{\mathcal{S}_i\}_{i=1}^{i=s}$ is defined as,

$$SSCV(\mathcal{C}, \{\mathcal{S}_i\}_{i=1}^{i=s}) = \sup_i \left| \frac{|\{j : y_j \in \mathcal{C}(X_j), j \in \mathcal{I}_i\}|}{|\mathcal{I}_i|} - (1 - \delta) \right|, \quad (16)$$

where $0 \leq SSCV(\mathcal{C}, \{\mathcal{S}_i\}_{i=1}^{i=s}) < 1$ is the maximum amount of deviation from the exact conditional coverage of $1 - \delta$ (i.e. worst case) in size-stratified sets $\{\mathcal{S}_i\}_{i=1}^{i=s}$ of prediction sets $\mathcal{C}(X)$. Note that in case of exact conditional coverage, the worst violation will be zero and $SSCV(\mathcal{C}, \{\mathcal{S}_i\}_{i=1}^{i=s}) = 0$. Thus, the lower SSCV represents higher adaptivity in prediction sets. RAPS is optimized to have the most adaptivity in coverage, i.e. the least SSCV, by choosing the optimal hyperparameter λ^* such that $\lambda^* = \arg \min_{\lambda} SSCV(\mathcal{C}, \{\mathcal{S}_i\}_{i=1}^{i=s})$.

We also propose our measure of quality in prediction sets incorporating both the coverage adaptivity and the average set size simultaneously to achieve a better judgement on the quality of prediction sets. We introduce a metric called *Size-Adaptivity Trade-off (SAT)* that increases when the average set size (reported in Tables 1 and 2) is decreased and/or the coverage adaptivity is increased (SSCV is decreased). Therefore, SAT score is inversely proportional to both the average set size $1 \leq \mu(\mathcal{C}) \leq K$ and the metric of adaptivity $SSCV(\mathcal{C}, \{\mathcal{S}_i\}_{i=1}^{i=s})$ computed in Equation (16). We define SAT score for the set-valued predictor \mathcal{C} and set-size ranges $\{\mathcal{S}_i\}_{i=1}^{i=s}$ as,

$$SAT(\mathcal{C}, \{\mathcal{S}_i\}_{i=1}^{i=s}) = \frac{1 - SSCV(\mathcal{C}, \{\mathcal{S}_i\}_{i=1}^{i=s})}{\mu(\mathcal{C})} \quad \text{s.t.} \quad \mu(\mathcal{C}) = \frac{\sum_{x \in \mathcal{X}_{val}} |\mathcal{C}(X = x)|}{\sum_{x \in \mathcal{X}_{val}} \mathbb{1}_{\{|\mathcal{C}(X=x)| > 0\}}}, \quad (17)$$

where $\mathbb{1}$ denotes the indicator function over non-empty prediction sets, and $0 < SAT(\cdot) \leq 1$ represents the quality of set-valued predictor \mathcal{C} . Note that as empty prediction sets have no practical information regarding the predictive uncertainty during deployment and a large number of empty sets can significantly reduce the average set size but without efficiency, we skip the empty prediction sets when computing $\mu(\mathcal{C})$ in Equation (17). In case of using a perfect classifier that is trained on infinite data and perfectly fit the true label for given input data, $SSCV(\mathcal{C}, \{\mathcal{S}_i\}_{i=1}^{i=s}) = 0$ due to the exact conditional coverage, and the model

produces prediction sets with the fixed size of 1 only containing the true label, i.e., $\mu(\mathcal{C}) = 1$; thus, the maximum SAT score is achieved, i.e. $SAT(\mathcal{C}, \{\mathcal{S}_i\}_{i=1}^s) = 1$. In our experiments, we partition the produced set sizes into 0 – 1, 2 – 3, 4 – 10, 11 – 100, and 101 – 1000 ranges. To apply RAPS method, we choose the optimal λ that yields to the smallest SSCV score out of the set of $\lambda \in \{1e-5, 1e-4, 8e-4, 1e-3, 15e-4, 2e-3, 1e-2, 0.1, 1\}$. In Table 5, we demonstrate the average SAT scores for ECP (the boldfaced columns) compared to other methods along with their corresponding SSCV value and set sizes considering different models. We also conducted further experiments to report and compare the adaptivity and the quality of prediction sets for ECP and Least Ambiguous Set-valued classifier (LAS) method in Appendix C.

Observations. We observe that ECP outperforms SoTA methods with SAT scores that are consistently higher than the other methods indicating that the prediction sets produced by ECP have noticeably higher quality rather than APS and RAPS. Practically speaking, higher SAT in ECP shows better trade-off between efficiency (set size) and coverage adaptivity as two conflicting criteria rather than SoTA methods. Although APS is an adaptive method with small SSCV scores similar to ECP, its SAT scores are significantly smaller than other methods due to high inefficiency (very large sets) and it also does not satisfy conditional coverage shown in Experiment 4.2 and Table 3.

When applying RAPS, we find the optimal λ where SSCV score for prediction sets is minimum. In practice, the optimal λ is usually small since RAPS produces larger sets when λ is smaller (light regularization) with near exact coverage, i.e. small violations from $1 - \delta$ coverage, conditional on size-stratified sets (see Table 4). This further optimization for addressing only one criterion (adaptivity) can also add computational burden compared to ECP method that is stable and free from hyperparameters. However, smaller SSCV scores in RAPS only imply on better adaptiveness which is not adequate for conclusion on the quality of prediction sets since the set size as a practical criterion is ignored. Therefore, unlike ECP, RAPS can be either optimized for smaller sets or more coverage adaptivity at a time. Although it gives us a flexibility to choose the required behavior, the desired prediction sets are the ones that consider all the three criteria, i.e. coverage, efficiency, and adaptivity, simultaneously. In case of conflicting criteria, a trade-off is required to produce prediction sets which is considered in ECP rather than SoTA methods, particularly the trade-off between set size and adaptivity. As shown in Table 5, we can see that although RAPS shows more adaptiveness with slightly smaller SSCV compared to ECP, RAPS significantly sacrifices the efficiency and shows larger sets. Thus, SAT scores for ECP are considerably higher rather than APS and RAPS by considering both adaptiveness and efficiency of prediction sets, simultaneously. This implies that the prediction sets produced by ECP is more practical having higher quality rather than the other methods.

5. Conclusion

In this paper, we have addressed the problem of model uncertainty in deep classifiers using conformal prediction. We used the model (epistemic) uncertainty derived from EDL as our heuristic notion of uncertainty along with evidential properties such as uncertainty surprisal and expected utility associated with the target labels, to propose a novel non-conformity score function. We applied our non-conformity score function to introduce evidential CP

(ECP) and produce efficient and adaptive prediction sets while maintaining the coverage of true labels. Our extensive experimental evaluations showed that ECP could outperform the SoTA CP methods in terms of efficiency (small set size) and adaptivity with no additional optimization process or computational burden.

Acknowledgments

We would like to express our sincere gratitude to the anonymous reviewers for their valuable comments, which greatly improved the quality of this manuscript. This research is supported by Natural Sciences and Engineering Research Council of Canada (NSERC) Discovery Grant RGPIN-2016-06062.

References

- Alexander Amini, Wilko Schwarting, Ava Soleimany, and Daniela Rus. Deep evidential regression. *Advances in Neural Information Processing Systems*, 33:14927–14937, 2020.
- Anastasios Angelopoulos, Stephen Bates, Jitendra Malik, and Michael I Jordan. Uncertainty sets for image classifiers using conformal prediction. *arXiv preprint arXiv:2009.14193*, 2020.
- Anastasios N Angelopoulos, Stephen Bates, et al. Conformal prediction: A gentle introduction. *Foundations and Trends® in Machine Learning*, 16(4):494–591, 2023.
- Arthur P Dempster. A generalization of bayesian inference. *Journal of the Royal Statistical Society: Series B (Methodological)*, 30(2):205–232, 1968.
- Yarin Gal and Zoubin Ghahramani. Dropout as a bayesian approximation: Representing model uncertainty in deep learning. In *international conference on machine learning*, pages 1050–1059. PMLR, 2016.
- Chuan Guo, Geoff Pleiss, Yu Sun, and Kilian Q Weinberger. On calibration of modern neural networks. In *International Conference on Machine Learning*, pages 1321–1330. PMLR, 2017.
- Kaiming He, Xiangyu Zhang, Shaoqing Ren, and Jian Sun. Deep residual learning for image recognition. In *Proceedings of the IEEE conference on computer vision and pattern recognition*, pages 770–778, 2016.
- Gao Huang, Zhuang Liu, Laurens van der Maaten, and Kilian Q. Weinberger. Densely connected convolutional networks. In *Proceedings of the IEEE Conference on Computer Vision and Pattern Recognition (CVPR)*, July 2017.
- Audun Jøsang. Subjective logic, 2016.
- Hamed Karimi and Reza Samavi. Quantifying deep learning model uncertainty in conformal prediction. In *Proceedings of the AAAI Symposium Series*, volume 1, pages 142–148, 2023.

- Samuel Kotz, Narayanaswamy Balakrishnan, and Norman L Johnson. *Continuous multivariate distributions, Volume 1: Models and applications*, volume 334. John Wiley & Sons, 2019.
- Balaji Lakshminarayanan, Alexander Pritzel, and Charles Blundell. Simple and scalable predictive uncertainty estimation using deep ensembles. *arXiv preprint arXiv:1612.01474*, 2016.
- Ningning Ma, Xiangyu Zhang, Hai-Tao Zheng, and Jian Sun. Shufflenet v2: Practical guidelines for efficient cnn architecture design. In *Proceedings of the European conference on computer vision (ECCV)*, pages 116–131, 2018.
- Jeremy Nixon, Michael W Dusenberry, Linchuan Zhang, Ghassen Jerfel, and Dustin Tran. Measuring calibration in deep learning. In *CVPR Workshops*, volume 2, 2019.
- Harris Papadopoulos, Kostas Proedrou, Volodya Vovk, and Alex Gammerman. Inductive confidence machines for regression. In *Machine Learning: ECML 2002: 13th European Conference on Machine Learning Helsinki, Finland, August 19–23, 2002 Proceedings 13*, pages 345–356. Springer, 2002.
- Tim Pearce, Alexandra Brintrup, Mohamed Zaki, and Andy Neely. High-quality prediction intervals for deep learning: A distribution-free, ensembled approach. In *International conference on machine learning*, pages 4075–4084. PMLR, 2018.
- John Platt et al. Probabilistic outputs for support vector machines and comparisons to regularized likelihood methods. *Advances in large margin classifiers*, 10(3):61–74, 1999.
- Yaniv Romano, Matteo Sesia, and Emmanuel Candes. Classification with valid and adaptive coverage. *Advances in Neural Information Processing Systems*, 33:3581–3591, 2020.
- Mauricio Sadinle, Jing Lei, and Larry Wasserman. Least ambiguous set-valued classifiers with bounded error levels. *Journal of the American Statistical Association*, 114(525): 223–234, 2019.
- Murat Sensoy, Lance Kaplan, and Melih Kandemir. Evidential deep learning to quantify classification uncertainty. *Advances in neural information processing systems*, 31, 2018.
- Glenn Shafer. *A mathematical theory of evidence*, 1976.
- Karen Simonyan and Andrew Zisserman. Very deep convolutional networks for large-scale image recognition. *arXiv preprint arXiv:1409.1556*, 2014.
- Christian Szegedy, Vincent Vanhoucke, Sergey Ioffe, Jon Shlens, and Zbigniew Wojna. Rethinking the inception architecture for computer vision. In *Proceedings of the IEEE conference on computer vision and pattern recognition*, pages 2818–2826, 2016.
- Ryan J Tibshirani, Rina Foygel Barber, Emmanuel Candes, and Aaditya Ramdas. Conformal prediction under covariate shift. *Advances in neural information processing systems*, 32, 2019.

- Sander Tonkens, Sophia Sun, Rose Yu, and Sylvia Herbert. Scalable safe long-horizon planning in dynamic environments leveraging conformal prediction and temporal correlations. In *Long-Term Human Motion Prediction Workshop, International Conference on Robotics and Automation*, 2023.
- Janette Vazquez and Julio C Facelli. Conformal prediction in clinical medical sciences. *Journal of Healthcare Informatics Research*, 6(3):241–252, 2022.
- Vladimir Vovk. Conditional validity of inductive conformal predictors. In *Asian conference on machine learning*, pages 475–490. PMLR, 2012.
- Vladimir Vovk, Alexander Gammerman, and Glenn Shafer. Algorithmic learning in a random world, 2005.
- Saining Xie, Ross Girshick, Piotr Dollár, Zhuowen Tu, and Kaiming He. Aggregated residual transformations for deep neural networks. In *Proceedings of the IEEE conference on computer vision and pattern recognition*, pages 1492–1500, 2017.
- Chong Zhang, Wenbo Wang, and Xingye Qiao. On reject and refine options in multiclass classification. *Journal of the American Statistical Association*, 113(522):730–745, 2018.

Appendix A. Proof of Theorem 8

Proof Following the belief and uncertainty quantification in EDL described in Section 3.1, we map the feature of Beta-distributed coverage to evidential setting to quantify the confidence and consequently, the uncertainty associated with the true label coverage. As Beta distribution is a Dirichlet distribution restricted by only two shape parameters (binomial version), we use evidential setting using a Beta distribution to form belief masses associated with each one of the parameters. Then, according to Equation (3), we can quantify the confidence (belief) of covering the true labels and the uncertainty associated with the coverage process. Formally, according to Equation (13), the two parameters for the Beta-distributed coverage are $\alpha_1 = n + 1 - l$ and $\alpha_2 = l$ representing the strength of Beta distribution in covering and miscovering the true label, respectively. Note that as Beta distribution has only two parameters α_1 and α_2 , we have $K = 2$. Here, we have $\alpha_0 = \sum_{i=1}^K \alpha_i = n + 1$ as the summation of Beta parameters. The evidence associated with these parameters represent the amount of support for covering the true label denoted by e_1 or miscovering the true label denoted by e_2 and calculated as $e_1 = \alpha_1 - 1$ and $e_2 = \alpha_2 - 1$, respectively based on Equation (1). Then, we can compute Beta parameters as $e_1 = n - l$ and $e_2 = l - 1$. Now, we compute the belief b_1 as the amount of confidence γ in covering the true label in the prediction sets on average corresponding to e_1 as,

$$\gamma = b_1 = \frac{e_1}{\alpha_0} = \frac{n - l}{n + 1} = \frac{n - \lfloor (n + 1)\delta \rfloor}{n + 1} . \quad (18)$$

Also, the uncertainty associated with the coverage is defined according to Equation (3) as,

$$U_c = \frac{K}{\alpha_0} = \frac{2}{n + 1} . \quad (19)$$

■

Appendix B. Efficiency of Prediction Sets When $\delta = 0.05$

In this section, we show the experimental results on the accuracy, average marginal coverage, and average prediction set size using different architectures and methods with $\delta = 0.05$ on both test sets ImageNet-Val and ImageNet-V2 in Tables 6 and 7, respectively (same observations and conclusions as stated in Section 4.1).

Appendix C. Adaptivity in Least Ambiguous Set-valued Classification

Least Ambiguous Set-valued (LAS) classification method (Sadinle et al., 2019) uses one minus the temperature-scaled softmax scores as its non-conformity function to find the optimal threshold and include the labels in the sets accordingly. In Table 8, we report SSCV as the adaptivity metric and SAT as the quality metric for both ECP and LAS along with their average marginal coverage and set sizes. We observe that both ECP and LAS produce small and highly efficient sets although having negligible differences in different models that are caused by stochasticity and finite validation dataset. However, unlike ECP, LAS sacrifices the set adaptivity by producing the smallest possible set sizes. In terms of

Table 6: Efficiency on **ImageNet-Val**: The median-of-means for marginal coverage and prediction set size using different architectures and methods with $\delta = 0.05$ over 10 trials

Model	Performance	Mean Marginal Coverage				Mean Prediction Set Size			
	Accuracy	Base	APS	RAPS	ECP	Base	APS	RAPS	ECP (Ours)
ResNeXT101	79.31%	0.937	0.950	0.950	0.950	36.09	45.73	4.14	3.11
ResNet152	78.31%	0.941	0.950	0.950	0.950	19.30	22.22	4.43	3.24
ResNet101	77.37%	0.945	0.951	0.950	0.951	19.62	23.31	4.87	3.83
ResNet50	76.13%	0.942	0.950	0.950	0.950	21.81	24.37	7.22	4.44
ResNet18	69.76%	0.944	0.951	0.949	0.950	28.85	31.44	13.65	8.85
DenseNet161	77.13%	0.939	0.950	0.950	0.950	24.65	25.68	5.06	3.78
VGG16	71.59%	0.945	0.950	0.901	0.950	25.31	28.69	11.10	6.73
ShuffleNet	69.36%	0.941	0.951	0.950	0.949	62.23	71.90	16.87	11.65
Inception	69.54%	0.946	0.951	0.950	0.950	138.43	171.52	19.32	10.96

Table 7: Efficiency on **ImageNet-V2**: The median-of-means for marginal coverage and prediction set size using different architectures and methods with $\delta = 0.05$ over 10 trials

Model	Performance	Mean Marginal Coverage				Mean Prediction Set Size			
	Accuracy	Base	APS	RAPS	ECP	Base	APS	RAPS	ECP (Ours)
ResNeXT101	67.51%	0.941	0.951	0.950	0.950	85.48	94.33	20.89	13.61
ResNet152	66.98%	0.943	0.949	0.950	0.951	52.90	57.07	26.30	11.36
ResNet101	65.54%	0.944	0.950	0.949	0.950	57.95	64.28	21.67	15.43
ResNet50	63.20%	0.936	0.950	0.951	0.950	62.08	69.21	29.53	17.09
ResNet18	57.29%	0.947	0.951	0.950	0.951	64.36	74.17	50.82	28.37
DenseNet161	65.13%	0.941	0.950	0.950	0.950	56.61	79.09	26.74	16.81
VGG16	58.81%	0.934	0.949	0.949	0.951	66.23	67.14	41.49	24.12
ShuffleNet	56.04%	0.937	0.951	0.949	0.950	136.52	143.00	92.51	47.89
Inception	57.59%	0.939	0.950	0.951	0.951	240.92	283.44	68.85	44.05

adaptiveness, ECP shows significantly lower SSCV compared to LAS that demonstrates lower deviations from the exact conditional coverage in ECP (lower coverage violation). Therefore, ECP has higher SAT scores compared to LAS indicating a considerably better trade-off between set size and adaptivity (higher quality) in the practical predictions.

Table 8: The performance and quality of prediction sets in LAS compared to ECP on ImageNet-Val data in different methods and model architectures with $\delta = 0.1$

Model	LAS				ECP (Ours)			
	Coverage	Size	SSCV	SAT	Coverage	Size	SSCV	SAT
ResNeXT101	0.900	1.65	0.150	0.511	0.900	1.65	0.072	0.560
ResNet152	0.901	1.75	0.141	0.490	0.900	1.76	0.077	0.520
ResNet101	0.900	1.85	0.147	0.465	0.899	1.83	0.076	0.486
ResNet50	0.900	2.04	0.131	0.426	0.900	2.06	0.092	0.439
ResNet18	0.900	3.65	0.207	0.216	0.900	3.66	0.075	0.254
DenseNet161	0.901	1.85	0.138	0.464	0.901	1.89	0.070	0.489
VGG16	0.899	2.97	0.202	0.267	0.900	2.95	0.067	0.308
ShuffleNet	0.900	4.05	0.196	0.198	0.900	4.06	0.138	0.228
Inception	0.900	3.96	0.185	0.205	0.900	4.05	0.132	0.242